ORGANIC SEMICONDUCTOR DEVICES

As electronic and optoelectronic devices become increasingly complex and the devices and materials from which they are made are pushed to their limits, novel devices or devices utilizing novel materials become increasingly attractive (1). In contrast to group IV (carbon, silicon, or germanium) or group III–V semiconductors which are inorganic materials (such as gallium arsenide, indium phosphide, gallium nitride), organic materials can be processed to possess properties ranging from highly insulating (conductivity $<10^{-12}$ S $\cdot$ cm^{-1}) to highly conducting (conductivity $>10^{5}$ S $\cdot$ cm^{-1}), and several such materials have been demonstrated. The fact that they are organic materials means that they are abundant and are relatively inexpensive.

Some organic materials such as a class of π-conjugated polymers, pentacene, thiophene oligomers such as α-hexathienylene (α-6T) have semiconducting properties in the neutral state and high electronic conductivity in the partially oxidized state. Thin films of these semiconducting polymers can be prepared by simple spin-casting of polymer solutions, affording simple fabrication of devices utilizing flexible films. However, the advantage of simplicity must be weighed against the inferiority of the electronic properties of current semiconducting polymers compared to the inorganic semiconductors. Currently, there is much work in developing a thorough understanding of the molecular, microscopic, and macroscopic properties of organic semiconductors. With this understanding, improved electrical or optical properties can be achieved by chemical modifications. This also allows the organic semiconductor devices to satisfy niche areas, some of which are described in this article. However, organic semiconductor devices are not expected to rival devices made using inorganic semiconductors for current electronic and optoelectronic applications.

Organic semiconductor devices have made significant progress in the last several years and are now being proposed as replacements for conventional semiconductor devices in a variety of areas including thin film transistors (TFTs), memories, photodiodes, solar cells, and light emitting devices (LEDs) for full-color flat panel displays. The organic materials used in these applications are light weight, flexible, conformable and are produced by simple manufacturing technologies, all of which make them potentially very inexpensive compared to inorganic semiconductor materials. Also, unlike inorganic semiconductors, for organic semiconductors, there is no need to grow a crystal, saw it, polish it, dope it, etc. It is processable in air, not in a chip-oriented processing environment. Organic semiconductor devices are potentially very inexpensive, can be fabricated with low temperature processing, and are a molecular engineering approach to electronics and optoelectronics.

This article concentrates on four types of organic semiconductor devices, and will present some of the latest results and fabrication technologies. Because of their huge commercial potential, a large part of the article describes and discusses light-emitting diodes (LEDs) made either with polymers or molecular organic materials (2,3). To improve the line width and enhance the efficiency of the LEDs, microcavities are discussed (4). For active display driver transistors and other applications, thin-film transistors with organic semiconductors and all-organic transistors are described (5–7). Finally, photovoltaic cells, photodiodes, and metal–organic semiconductor junctions are described (8,9).

LIGHT-EMITTING DIODES

Light-emitting devices (LEDs) are made from thin layers of organic or polymer materials as the electroluminescent (EL) material (10–21). Electroluminescence is the emission of light as a result of the application of an electric field. These LEDs constitute an enabling technology for fabricating flexible, full-color, emissive displays. They are also being proposed for other "small-scale" applications, such as simple backlights, alphanumeric displays, displays for car radios, and small handheld devices and toys, larger panel displays for home appliances, stereo equipment, automobile dashboards, and matrix addressable panel displays, such as in notebook computer screens. Their advantages include very high resolution of few micron size pixels and any size and shape of pixels; fast switching speed corresponding to delay times below microseconds, so video display capability is possible; low voltage operation below 3 V for battery-operated applications; very high contrast; high internal quantum efficiency (defined as the number of photons generated per electron-hole pair injected) of up to several percent; very high brightness of several thousands candelas per square meter; very light weight for portability; easy processability on flexible substrates and large area coating; and ruggedness. Note that all these advantages are not available in any single device; rather they represent the advantages available from a variety of LEDs.

The device design is quite simple, and the cost and consumption of materials is low, thus making manufacturing quite inexpensive. It is also possible to fabricate large displays with good mechanical flexibility. The technology is emissive with lambertian characteristics, which means that a 180° viewing angle is possible. The size, thickness, durability and ruggedness, flexibility, and formability of the organic or polymer LEDs are in principle limited by the type of substrates used. Typical substrates are thin sheets of glass, sheets or rolls of plastic, or metal foil.

These light-emitting diodes are either based on molecular organic materials or on polymers as the electroluminescent material. The organic materials used in the electroluminescent devices may be classified according to their molecular structure into the following three categories: organic dyes with no metal elements; chelate metal complexes or small organic molecules as opposed to long polymer chains (also called molecular organic materials); and conjugated polymers (17).

Examples of organic dyes with no metal elements include derivatives of oxadiazole, distyrylaryl, phenylamine, phthaloperinone, quinacridone, pyrazoline, and metal-free phthalocyanine. These dyes have high quantum yield, easily film for-

mation by vacuum vapor deposition, high purifying capability and a variety of material designs. However, they suffer from easy crystallization after film formation, and occasionally produce exciplexes with other organic materials, and so are not widely used.

As discussed later, at present, the small molecule approach for LEDs (11,16) has some advantages in brightness and demonstrated lifetime, but the polymer approach is advancing very rapidly. The polymer approach (light-emitting polymers or LEPs) is less sensitive to high temperatures and is less costly since LEPs can be made by spin-casting on substrates and the electrodes can be printed on films with roll-to-roll coating machines at very low cost and in very large sizes. In contrast, LEDs with small organic molecular films (called organic LEDs or OLEDs) must be vapor deposited.

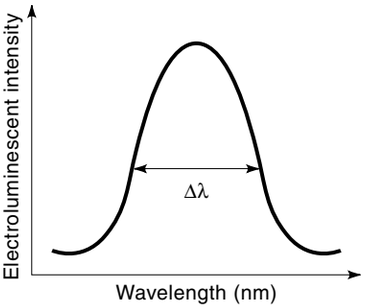

Figure 2. Schematic representation of the spectrum of light emitted from an OLED. The spectrum is broadened ($\Delta\lambda$) due to vibronic coupling that is characteristic for optical transitions in semiconductors in which the excited state is a singlet.

ORGANIC LIGHT-EMITTING DIODES (OLEDs)

Examples of chelate metal complexes and small organic molecules are tris-hydroxyquinolinate aluminum (Alq_3) and azomethine metal complexes. When bis(10-hydroxybenzo[h]quinolinato)-beryllium ($BeBq_2$) is used as the electron transporting layer with Alq_3, excellent EL properties are obtained from these OLEDs.

OLEDs are projected to be the replacement technology for cathode ray tubes (CRTs) and liquid crystal displays (LCDs) because of their brightness, high resolution, energy efficiency, and cost effectiveness (16). As flat panel indoor or portable displays, these OLEDs must be sufficiently bright (>100 cd/m^2), have good quantum efficiency and high electrical efficiency (low voltage between 5 V and 15 V, and low current operation), have good color saturation, and long lifetimes (>10,000 h).

Figure 1 shows the basic single heterostructure OLED which consists of two organic semiconductor layers deposited on a transparent anode on a substrate. A typical emission spectrum from an OLED is shown in Fig. 2. In the OLED, the first organic layer is the hole-transporting layer, and the second is the electron-transporting and light-emitting layer, on top of which is deposited a suitable cathode. A forward bias voltage is applied across the anode–cathode electrodes. The cathode and anode provide negative and positive charge carriers which recombine and form bound excited states (excitons) which can decay radiatively in the luminescent organic semiconductor to emit light through the transparent electrode and substrate. The construction of pixels and patterning of the emission layer is simply achieved by patterning the electrodes because the electroluminescent polymers normally have very high resistivities, thus minimizing cross talk and charge carrier transport or diffusion between pixels.

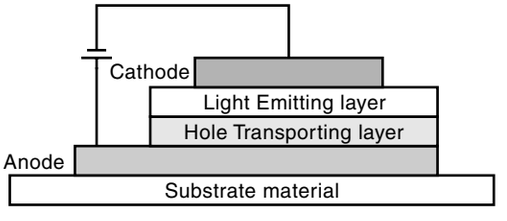

Figure 1. Schematic representation of the basic structure of an organic light-emitting diode (OLED). The two organic hole transporting and electron-transporting/light-emitting layers for an organic single heterostructure, whose band diagram is shown in Fig. 3.

To construct the electrodes, a thin layer of indium tin oxide (ITO) is used as the anode because it is transparent. A hole injection/buffer layer of copper phthalocyanine can be used between the anode and hole transport layer to improve the interfacial quality. The cathode is made of a suitable metal or alloy that is a low work function material to make it easier for electron injection into the organic materials. However cathodes using low work function metals are highly reactive, and the electroluminescent cells are often damaged, so that Al–Li alloy is often used as cathode, although it is difficult to evaporate. Other cathode materials include MgAl and LiF/MgAl alloys.

Small amounts of dyes in the hole and electron-transporting layers (e.g., poly(*N*-vinylcarbazole) (PVK)/Alq_3) are thought to function as efficient emission centers either by carrier trapping electron and holes to form excitons, or by energy transfer by trapping excitons formed on Alq_3. Organic material-polymer PVK doped with electron transport agents and a dye gives brightness >10^4 cd/m^2 (18). Examples of molecules used as hole-transporting layers are triphenyl dimamine (TPD) or 4,4′-bis[*N*-(1-napthyl)-*N*-phenyl-amino]biphenyl (α-NPD). For the light-emitting/electron transport layer, bis(8-hydroxy)quinaldine aluminum phenoxide ($Alq_2'OPh$), tris(8-hydroxyquinoline) aluminum (Alq_3), or 5,10,15,20-tetraphenyl-21H,23H-porphine (TPP) are used.

For practical applications, the device efficiency η_{device}, defined as

$$\eta_{\text{device}} = \gamma \cdot \eta_{\text{electron-hole}} \cdot \Phi_{\text{fluorescence}}$$

is very important. Here, γ is the ratio of minority to majority carriers. It is related to the carrier injection process and depends on the electrodes used. $\eta_{\text{electron-hole}}$ is the electron-hole recombination efficiency and is related to both the materials used and to the device structure. $\Phi_{\text{fluorescence}}$ is the fluorescent efficiency of the light-emitting material. Because carriers are injected into the LED with uncorrelated spins, only 25% will recombine as molecular singlet states, assuming statistical branching between singlet and triplet states. So the maximum value of $\Phi_{\text{fluorescence}}$ is 25%.

Variations of the simple, single-heterostructure OLED include an organic three-layer double-heterostructure in which separate electron-conducting and light-emitting layers are de-

posited on top of the hole-transporting layer. Variations in color emitted depend on the chemical composition or on the type of dye incorporated into the organic light-emitting material. For example, $Alq_2'OPh$ is commonly used for blue light, Alq_3 for green light, and TPP for red light.

Full color OLEDs can be made in several architectures (11). The first is side-by-side patterning of red, green, and blue OLEDs in which each color OLED is sealed with a metal layer to prevent degradation of the organic materials when exposed to solvents and water during patterning of films and microfabrication processing. In this approach, each color OLED uses a different organic film and the structure is a planar array of OLEDs in which each OLED is similar to that shown in Figure 1.

A second approach is to use white OLEDs, made by depositing two or more organic layers or combining layers of different blends, with passband filters for red, green, and blue. However, the inefficiency of the color subtraction process, which requires that each OLED be driven to much higher brightness at higher voltages and currents, also results in increased power consumption and degradation of reliability.

A third approach is to use microcavity-based filters which are described in detail later. In this approach, the emitted wavelength is direction-dependent. To reduce this color directionality, designs are refined by using scattering layers outside the microcavity. However, this reduces the efficiency of the OLED.

A fourth approach is to use color tunable OLEDs in which each color is obtained by varying the applied voltage. Higher voltage biases across the OLED results in emission from high excitation energies and higher frequencies (blue shifts). The higher voltages result in increased brightness and power consumption but enhanced degradation.

This fourth approach could be used to make stacked organic LEDS (SOLEDs) by stacking of color pixels on top of each other instead of the conventional side-by-side configuration. The advantage of this technology is that it provides three times the resolution in the same area, and it is suited to high definition televisions (HDTVs) on flat panel displays that hang on a wall like paintings, cellular phones, laptop computers, and other portable devices with bright displays that consume considerably less energy. However, the potential problems are reduced efficiency due to absorption in the semitransparent electrodes and color bleeding by the red emitting layer caused by energy down-conversion of light emitted from the blue element.

The organic materials typically used in OLEDs undergo detrimental reactions with oxygen and/or water when they are in excited states either through exposure to UV/visible light or while being operated. Therefore, a key basic requirement for OLEDs is that the organic materials must be protected from oxygen or moisture when they are in excited states. In addition, they should also be stable over the required product shelf life which is typically more than five years. This means that the OLEDs must be appropriately protected and encapsulated (19). It was found that if light of energy above the band gap of the molecular organic semiconductor is excluded by a high energy cut-off filter, then the stability of the polymer against photodegradation in oxygen or moisture is greatly reduced. However, this filter reduces emission efficiencies. Corrosion of the cathode and degradation of the electrode/organic material interfaces also results in degradation of the OLEDs even when light above the band gap of the polymer is excluded.

The quality and electronic properties of the substrate/anode interface, the cathode, and the organic layers are crucial for good device performance. Because of this, much research is being done to study the work functions of the electrodes; the smoothness, adhesion, and resistance to corrosion of the metal films, enhancement of reliability and efficiency of the organic layers; stability of the organic layers, and encapsulation techniques. The desired characteristics (20) are suitable ionization potential and electron affinity for energy level matching in the injection process of charge carriers at the electrode to organic materials and organic material to organic material interfaces; uniform amorphous films without pinholes; morphological stablility without crystallization during processing; thermal stablility without morphological changes or melting from Joule heating during the operation of the device; and emissions that are highly fluorescent.

Areas of continuing research in organic light-emitting diodes are now described. Crystallinity or instability in organic EL diodes is one of the problems which must be overcome because it limits device lifetime. Improved efficiency of electrical to optical energy conversion required for battery operation for long periods and good chromaticity are required. A complete understanding of the degradation mechanisms and ways to overcome them are required so that these devices would have lifetimes comparable to those of computers and TVs, which is expected by consumers.

LIGHT EMITTING POLYMERS

Examples of conjugated polymers (10,12–14) are poly(*p*-phenylenevinylene) (PPV) and some of its derivatives, polythiophenes (PT), poly *p*-phenylenes (PPP), polyphenylene ethynylene (PPE), polyanilene, polypyrrole, polypyridines, polypridyl(vinylenes), and copolymers of these materials. Electroluminescent diodes made from conjugated polymers are often called light emitting polymers (LEPs) or polymer LEDs (PLEDs). A key attraction of polymer LEDs compared to the other organic EL technologies is the ease with which the polymers can be processed and in particular coated without crystallization, but purification is sometimes difficult.

Early LEPs (13) were based on PPV, PPP, and PT which emit in the green, blue, and red bands, respectively. These conjugated polymers are used as electroluminescent materials, and LEDs based on them offer the attractive possibility to tune the color of light by appropriately modifying the chemical structure. For example, for PPV whose structure is shown in Fig. 3, depending on its degree of conjugation or conjugation breaking and the presence of electron donating or accepting side groups in both the phenyl and vinyl groups, the band gap and emission color can be varied from blue to red. Another approach is to synthesize copolymers with fluorescent blocks of defined lengths which are separated by nonconjugated spacers into the polymeric main chain or by nonconjugated polymers with fluorescent dyes in the side chains. In this way, precise adjustment of the color emitted is obtained.

Conjugated polymers, one of the most popular class of EL materials, are quasi one-dimensional electronic systems with semiconducting properties that arise from the overlap over several sites of the p_z orbitals originating from the double or

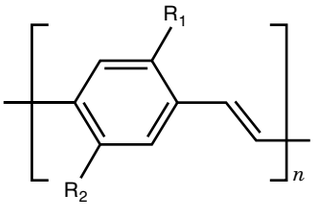

Figure 3. Schematic representation of the structure of PPV-based conjugated polymers. Without the side groups R_1 and R_2, this is PPV. These polymers have semiconductor-like electron configurations, and their macromolecules contain alternating single- and double-bond systems. The π-electrons are delocalized over the entire molecular chain. Variation of the side groups R_1 and R_2 changes the chemical, electrical, and optical properties. For example, for MEH-PPV, R_1 = $OCH(C_2H_5)C_4H_9$ and R_2 = OCH_3.

triple bonds. This overlap leads to the formation of well-delocalized π valence and π^* conduction bands. Their optical band gap depends on the planarity of the conjugated polymer backbone, and the band gap determines color in both emission and absorption. By substituting side-chains in the main polymer chain, it is possible to control the electronic, optical, and chemical characteristics of the conjugated polymer. These side chains attached to the conjugated polymer main chain also provide tunability of the band gap. The conductivity of the conjugated polymers is adjustable, and color tuning is simpler than with organic metal complexes or molecular organic materials.

PPV is a π-conjugated polymer with an energy gap between the π–π^* states of ~2.5 eV, and it produces luminescence in a band below this energy. PPV is an intractable material with a rigid-rod microcrystalline structure which gives rise to excellent mechanical properties with high elastic modulus and thermal stability. It is infusible and insoluble in common solvents, and so it is prepared by a precursor route in which a solution-processable nonconjugated precursor polymer is processed into the desired form and then converted into the conjugated polymer by thermal treatment. The properties of the resulting PPV depend on the synthesis of the material, the conditions of conversion, and how the samples are stored.

PPVs which are used as the EL material do not have glass transition temperatures and are stable at more than 400°C. This thermal stability is considerably higher than that of molecular organic materials used in OLEDs. The insolubility of the PPV films means that other layers may be wet processed without affecting their integrity. They are also hard enough to withstand sputtering of the final electrode. In addition, polymer LEDs offer low voltage operation, a large emissive area, a range of colors, and physical flexibility. For example, luminescence comparable to television screens (~100 cd/m^2) are routinely obtained at drive voltages less than 5 V.

Figure 4 shows a simple LEP structure. Although not widely used for major applications, this structure is a good vehicle for organic semiconductor testing because of its simplicity and the fact that it has only a few interfaces. Single-layer devices are typically fabricated on glass coated with ITO. First, the precursor, for example, a PPV polyelectrolyte precursor consisting of a random copolymer with acetate side groups and tetrahydrothiophenium groups with bromide counterions and a water/methanol mixture as the solvent is spin-coated onto the ITO-coated glass substrate. Polyethylene terephthalate (plastic overhead transparency) is also used as a substrate material. Then this spin-coated film is thermally converted to a dense pinhole-free PPV copolymer film which consists of conjugated PPV segments and a nonconjugated α-acetyloxy-*p*-xyleylene units, by heating at 150°C in pure nitrogen for 1 hour to 4 hours. Poly[2-methoxy-5-(2′-ethylhexyloxy)-1,4 phenylenevinylene] (MEH-PPV), a semiconductor with a band gap of 2.1 eV, is also used as the electroluminescent layer. Then calcium cathodes, which degrade rapidly in air and so must be protected rigorously, or cathodes of an aluminum alloy of low work function to reduce turn-on voltage, are sputter deposited. Sputtering produces pin-hole free films that have good adhesion and compact, small grain-size morphology, and it is a high-throughput deposition method. It can also easily deposit alloys of well-defined composition.

Adding a thin layer of conducting polymer [polyethylene dioxythiophene/polystyrene sulfonate (PEDOT/PSS)] by spin-coating between ITO and PPV reduces ITO/PPV precursor interaction and improves the device′s efficiency. The high electroluminescent efficiency results partly from high polymer purity which is an important factor for long-term stability. Ionic impurities, which can cause undesired drift effects in the device or initiate photochemical reactions, are removed to levels below 10 ppm by dialyzing the precursor, which also removes low molecular weight compounds. The presence of oxygen in the films during and after thermal conversion from precursor to conjugated polymer may cause the formation of carbonyl groups which may quench luminescence and trigger chain scission reactions. Water may also enhance photochemical degradation of the polymer and corrosion of the cathode. Thus LEPs must be encapsulated.

For single polymer devices, reducing the barrier to electron injection by using cathodes with a low work function improves the efficiency, but usually such low work function metals (Ca, for example) are unstable in air (21). Alternatively, double-layer polymer structures similar to that shown in Fig. 1 improve the efficiency without using unstable electrodes. Electroluminescence is maximized by balancing the injection of electrons and holes (determined by the barrier heights at anode and cathode and carrier mobilities), increasing the likelihood of electron/hole capture to form excitons, and luminescent efficiency. The barrier height between ITO and PPV does not limit hole injection. The LEP's characteristics in the low and medium voltage range are determined by the injection properties of the electrodes. At higher voltages (higher current densities), a transition from electron-limited injection to bulk-limited conduction occurs.

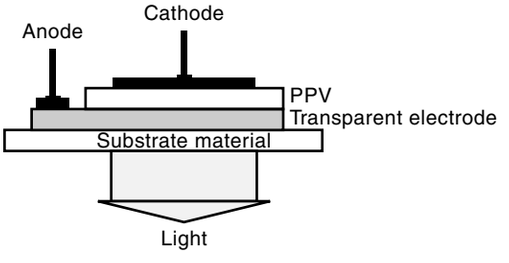

Figure 4. Schematic diagram of a single-layer light-emitting diode which works only under forward dc bias for electroluminescence.

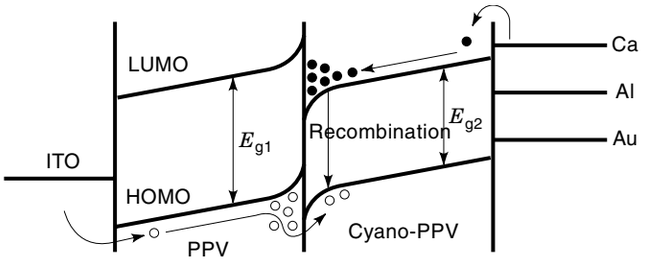

Figure 5. LEP fabricated with a heterostructure of PPV and CN-PPV of typical total thickness ~100 nm. The band gaps and work functions of the polymers can be tuned by organic synthesis. Under forward bias, holes (open circles) are injected from ITO into the highest occupied molecular orbital (HOMO) of the PPV layer and then drift to the heterointerface. Electrons (closed circles) are injected from the negative electrode into the lowest unoccupied molecular orbital (LUMO) and are confined to the heterointerface as shown. Thus a space charge is on either side of the heterojunction, and tunneling across the lower of the two barriers (holes in this case) leads to electron-hole capture and electroluminescence.

For a stable elemental cathode, the barrier height to electron injection should be >1 eV, and this is the limiting factor to the device's efficiency. This is overcome with a low work function alloy of aluminum to maximize electron injection efficiency and with recombination occurring in the PPV material. Using a PPV precursor of high luminescent efficiency, an ITO protector layer to prevent quenching of the luminescence due to interaction of conversion by-products with the ITO, and a low work function stable alloy of Al, devices with >2 lm/W and a peak brightness of >90,000 cd/m^2 have been produced.

In many LEP structures, a hole-transport layer is used between the anode and the EL layer, and an electron-injecting and transporting layer, such as 2,4-(biphenyl)-5-(4-*t*-butylphenyl)-1,3,4-oxadiazole (PBD) or poly(phenylene-1,2,3,4-oxadiazole-phenylene-hexafluoroisopropylidene) (PPOPH) ~10 nm thick is used between the EL layer and the metal cathode. These injecting layers serve the following functions: enhancing charge carrier injection; avoiding the quenching of radiative recombination near the metal interface, and balancing charge carrier injection. The net result is a significant increase in quantum efficiency.

Another improved version of the single layer LEP includes a cyano-PPV (CN-PPV) layer which functions as an electron-transport layer. In this structure, the electron and hole injection barriers are similar. The band gap of the CN-PPV film (~2.1 eV) is lower than the PPV layer (~2.5 eV), so recombination takes place in the CN-PPV layer. The band structure for this LEP is shown in Fig. 5. The switching speeds of these devices are quite fast even though the carrier mobilities in the 100 nm thick PV are low. With carrier mobilities in the 10^{-4} cm^2/Vs range and an electric field of 10^5 to 10^6 V/cm, drift times τ of less than 1 μs, given by

$$\tau = \frac{\text{film thickness}}{\text{carrier mobility} \cdot \text{mean electric field}}$$

are obtained. These drift times across the thin layers are less than the RC charging time of the dielectric structure, so the relatively low mobilities are unimportant.

Use of conducting polymer polyaniline (PANI) doped with camphor-sulfonic acid (CSA) spin-casted on top of the indium tin oxide (work function ~4.1 eV) film enhances the light output and reduces the operating voltage. Further, PANI-CSA films (~50 nm thick and work function ~4.3 eV) can also be used as the transparent electrode and an efficient electron injecting layer, thus simplifying the device's structure and fabrication. The main advantages of polymers as the EL materials in LEDs are easy film deposition by casting and no crystallization, but purification is sometimes difficult. For example (2), ITO/PANI-CSA/MEH-PPV/Ca LEPs have the following brightness characteristics: 100 cd/m^2 at 2.4 V (the brightness of a television screen); 4,000 cd/m^2 at <4 V (the brightness of a fluorescent lamp); and >10,000 cd/m^2 at >5 V biases. The external quantum efficiency is 2% to 2.5% photons/electrons and the luminous efficiency is 3 lm/W to 4.5 lm/W (2).

Adding 3 nm self-assembled monolayers of PPV thin films at the PPV/aluminum interface improves device efficiency by as much as a factor of 5 in light-emitting multilayer heterostructures. These self-assembled monolayers (SAMs) reduce the electron metal/organic Schottky barrier height when they form dipole layers on the metal contacts with the dipole moment pointing away from the metal substrate (electric field pointing toward the substrate). These nanometer-sized semiconductor particles on top of the hole-conducting polymer layer also control the color of light emitted by a LED because the color of light emitted depends on the size of the particles. More research is needed for LEDs using this technique for tuning color and enhancing efficiency.

Conjugated polymers should possess suitable ionization potential and electron affinity for energy level matching in the injection process of charge carriers at the electrode to organic material and organic material to organic material interfaces (51). They should form uniform amorphous films without pinholes and be morphologically stable without undergoing crystallization. The materials should also be thermally stable without morphological changes or melting by Joule's heat during the device's operation, and they should be highly fluorescent. Although there has been much progress in addressing these issues, there is still room for improvement if these LEDs are to find widespread use as forecasted.

Degradation during electrical stress from an increase in operating voltage probably due to the motion of ions through the device, a decrease in quantum efficiency, formation of dark spots which is greatly accelerated by the presence of water and the formation of electrical shorts must be minimized or eliminated. Power dissipation is very important because it leads to self-heating of the display. Ability to integrate different organic layers for optimum R, G, and B devices for color, and unbreakable substrates (as opposed to glass) are highly desirable. Integration of amorphous silicon TFT with a single organic layer structure OLED on flexible stainless steel foils for active matrix architecture has been demonstrated. This yields a display with far higher power efficiency than passive matrix addressing displays. However, more research is required to improve fabrication yield.

Polymer Microcavities

Two types of light emitting devices, OLEDs and LEPs, have been described. However, the spectra of such devices are gen-

erally very broad because of vibronic side bands and strong inhomogeneous broadening of the transitions (22). One way to spectrally narrow and resonantly enhance the broadened linewidths is to use Fabry–Perot resonant microcavities. A microcavity can be formed with a silicon dioxide/silicon nitride (or TiO_2/SiO_2) distributed Bragg reflector (DBR) and a metal mirror (4). A cavity structure with the conjugated polymer poly(2,5-dialkoxy-*p*-phenylenevinylene) (PDAOPV) (22,23) is schematically shown in Fig. 6. Other organic materials, such as PPV (24,25) and tris(8-hydroxyquinolinol)aluminum (Alq_3) (26) can also be used.

In this microcavity structure, the aluminum layer on top of the Si_xN_y filler layer is semitransparent. It is 13 nm thick, and it serves as the cathode. ITO can also be used as the cathode. A gold, aluminum, or indium mirror serves as the anode. Because the mobility of holes is greater than that of electrons, most of the electroluminescent emission occurs near the polymer/Al interface. If the ITO/PDAOPV/Al structure is used, then a broad spectrum at 592 nm that has a full-width at half-maximum (FWHM or $\Delta\lambda$) of 112 nm, as schematically depicted in the upper part of Fig. 7, is obtained. With the microcavity structure, the EL peak shifts to 634 nm and the FWHM is 34 nm, as shown in the lower part of Fig. 7. However, there is some angular variation of the emission color.

Other variations of the cavity structure include a top mirror (aluminum), an organic luminescent material, such as Alq_3 on top of a triphenyldiamine derivative (TAD) for the hole transport layer, a thin semitransparent layer of gold, a filler layer of transparent polyimide (27), and a quarter-wave stack of alternating layers of dielectrics (SiO_2/Si_xN_y) of low and high dielectric refractive indexes on top of a quartz substrate. The filler layer of polyimide is used to control the optical thickness and thus the spectral position of the electromagnetic cavity modes of the entire cavity without changing the properties of the luminescent layer. In this way, emission of red, green, and blue light is obtained by using different thicknesses of the filler layers.

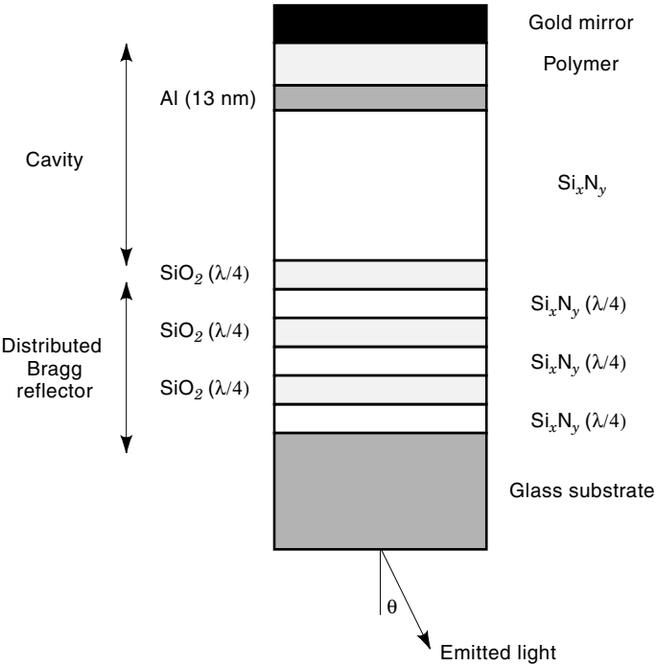

Figure 6. Schematic illustration of an electroluminescent microcavity polymer LED structure. In this structure, the wavelength of the emitted light depends on the viewing angle θ.

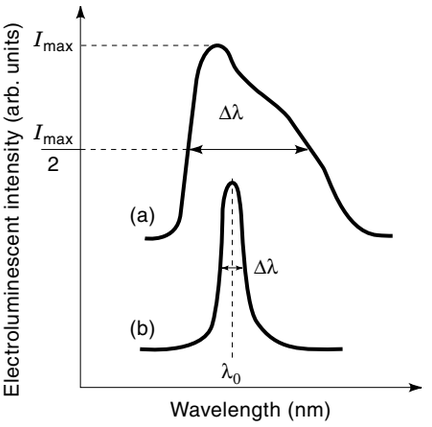

Figure 7. Electroluminescence spectra from a polymer LED (a) without and (b) with a microcavity. The microcavity considerably reduces the emission linewidth and shifts the emission wavelength. The emission wavelength depends on the geometrical distance between the mirrors, the refractive indices of the materials between the mirrors, the phase shifts at the mirrors, the cavity mode number, and the observation angle. For example, in (24), for a PPV-based LED, the bandwidth of the freespace spectrum LED is 150 nm, starting at 500 nm. With the microcavity structure, the peak wavelength was 584 nm and its bandwidth was 4 nm. The quality factor of this microcavity structure was 146.

Microcavities of high quality factor Q where $Q = \lambda_o/\Delta\lambda$ (see Fig. 7), have also been used to study the nature of emission from conjugated polymers, such as PPV (24). It was found that the main photoexcitation in PPV is an emissive intrachain exciton which could be exploited for electrically driven polymer-based lasers. Because Q depends on the mirror and DBR reflectivities and the effective mode number of the cavity, then high Q's can be obtained by using highly reflecting metal and DBR mirrors. With high Q cavities, measured FWHM were only a few nm, indicating that polymers of high quality can be used in electrically pumped lasers. By adjusting the optical parameters (wavelength and spectral width) of the cavity, it is possible to tune the color of the cavity emission over the entire polymer's spectrum. The planar structure of the polymer device also leads to spatial narrowing of the cavity mode's emission. Therefore, the microcavity structure allows one to control the process of radiative recombination in polymer luminescent materials, thereby significantly narrowing the spectral and spatial emission and also enhancing the forward emission intensity. However, more research into optical cavity designs that produce strongly directed emission is required.

ORGANIC THIN FILM TRANSISTORS

Work in organic thin-film transistors (OTFTs) (1,5–7,28–42) has been spurred on by the rapid growth in display technology that requires transistors for accessing individual display elements in the active matrix flat panel liquid crystal or organic emissive displays and in low-cost electronic applica-

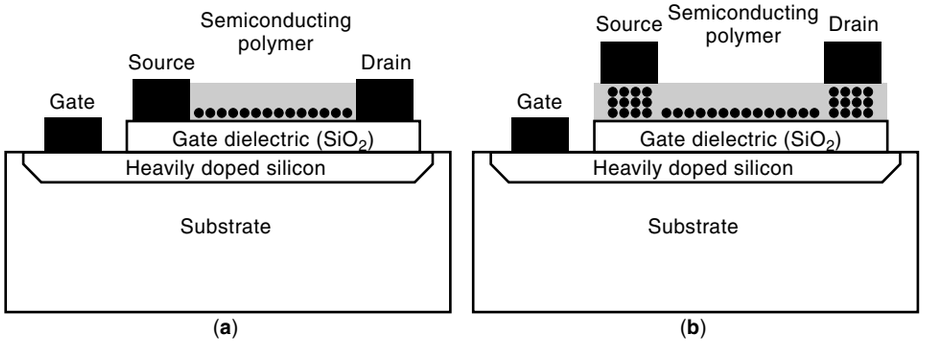

Figure 8. Simple schematic illustration (a) bottom contact and (b) top contact OTFT or MISFET. The dots in both figures indicate the charge carrier flow path between the source and drain terminals.

tions, such as low-end data storage, smart cards, or smart inventory or identification tags. These OTFTs or metal-insulator semiconductor field-effect transistors (MISFETs) possess the important advantage of being more readily deposited or spin cast onto rugged substrates, for example, various plastic ones, compared with amorphous and polysilicon TFTs. In addition, polymeric substrates can be used to make flexible form-factor displays and the OTFTs could also be manufactured by continuous web processing which dramatically lowers production costs.

The organic TFTs can be classified into two main structures: a bottom contact or a top contact device, as shown in the Fig. 8. Typical subthreshold characteristics at a constant drain voltage and drain current-drain voltage curves at varying gate voltages are shown in Fig. 9. The current voltage expressions for the TFTs are given by

$$I_{DS} = \mu \cdot C_{OX} \cdot \frac{W}{L} \cdot \left((V_{GS} - V_T) - \frac{V_{DS}}{2} \right) \cdot V_{DS}$$

in the linear region $(V_{GS} - V_T) > V_{DS}$ and

$$I_{DS} = \frac{\mu \cdot C_{OX}}{2} \cdot \frac{W}{L} \cdot (V_{GS} - V_T)^2 \cdot (1 + \lambda V_{DS})$$

in the saturated region $(V_{GS} - V_T) < V_{DS}$

where μ is the carrier field-effect mobility, C_{OX} is the gate oxide capacitance per unit area, and W and L are the channel width and length, respectively. V_{GS} and V_{DS} are the gate-source and drain-source biases, λ is the channel length modulation factor, and V_T is the "threshold voltage." These expressions are identical to those for describing inorganic field-effect transistors.

The top contact device offers simpler processing and results in higher mobilities because of easier charge injection from the top contacts. However, the bottom contact devices are necessary in making integrated circuits. Bottom contact devices generally have poorer performance which is improved by depositing the organic semiconductor at higher temperatures, but this degrades film morphology. A better technique is to use a high temperature deposited layer over which another layer deposited at a lower temperature is placed to improve the performance of bottom contact TFTs. Using stacked high-temperature and low-temperature layers of pentacene, record mobilities of 1.5 cm^2/Vs are obtained.

Organic insulator to organic semiconductor FETs have also been fabricated from polymer materials by printing techniques. These MISFETs are insensitive to deformations, such as bending or twisting. The substrate, a 25 μm thick polymer film made from poly(*p*-banic acid) resin (PPA) was used because of its good mechanical strength. The gate insulator was cyanoethylpullulan (CYEPL). Gold was used for the gate and source and drain electrodes and α-hexathienylene (α-6T) was the semiconductor. For this structure with an improved organic semiconductor to organic insulator interface, field-effect mobilities as high as 0.43 cm^2/Vs and carrier transit times of 5 μs are obtained.

Logic gates and ring oscillators with five inverter stages, made with either pentacene or poly(thienylenevinylene) (PTV) have been produced, indicating that OTFTs with good reproducibility for logic circuits can be manufactured (32). However, for circuits with only π-channel TFTs, a positive de-

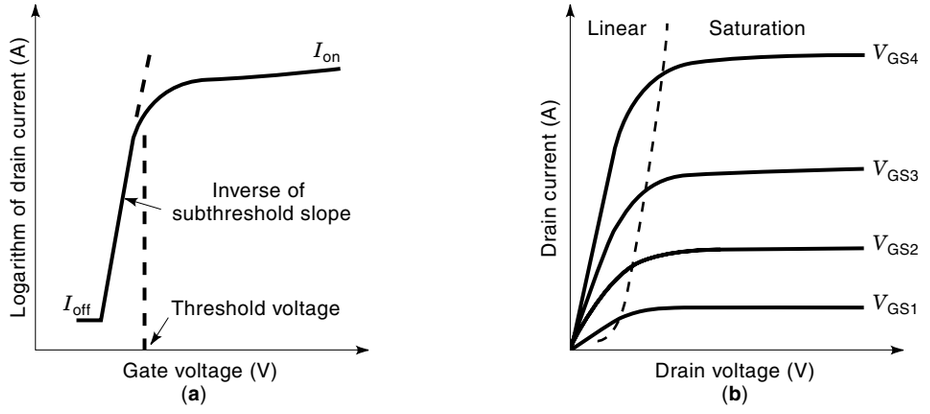

Figure 9. Schematic illustration of (a) subthreshold (I_{DS}–V_{GS}) at a constant drain voltage. The gate voltage range is typically 100 V to −100 V and the drain current is from 10^{-12} A to 10^{-4} A (37). (b) I_{DS}–V_{DS} characteristics at varying gate voltages increasing from V_{GS1} to V_{GS4}. I_{DS} is typically from 0 to −120 μA for V_{DS} from 0 to −10V and the V_{GS1} to V_{GS4} are 0, −10 V, −20 V and −30 V, respectively. In (b), the linear and saturation modes of operation are indicated.

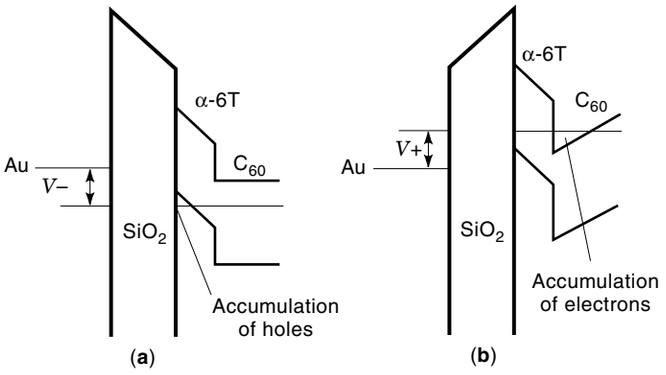

Figure 10. Schematic illustration of a heterostructure with (a) *P*-channel enhancement FET with a negative bias to gate and (b) *N*-channel enhancement FET with a positive bias to gate. Here, it is assumed that the magnitudes of the energy band level discontinuities at the heterojunction are not affected by the voltage bias. Also, it is assumed that the interface state densities at both interfaces are quite low, so little or no band bending of the energy levels occurs.

vice threshold means that a carrier accumulation layer and current leakage path can exist between circuit wiring elements. For *n*-channel devices, copper phthalocyanine and naphthalene tetracarboxyclic dianhydride (NTCDA) can be used as the organic semiconductor (35).

Organic heterostructure bottom contact field-effect transistors using α-6T and C_{60} as the heterostructural layers and working either as *n* or *p*-type devices depending on the gate bias, as shown in Fig. 10, have been produced (28). The electrical characteristics of these FETs depend mainly on the molecular orbital energy levels and transport properties of the two organic semiconductors. As a *p*-channel transistor, an accumulation of holes is formed at the α-6T-SiO_2 interface, whereas as an *n*-channel transistor, an accumulation layer of electrons is formed in C_{60} near the α-6T interface.

The operation of these heterojunction transistors also sheds light on the reason that many organic semiconductors conduct only one type of carrier species efficiently at room temperature: the other species are trapped in extremely low mobility states. These heterojunction transistors can be used to fabricate complementary circuits for low-power digital applications, such as smart cards or smart inventory tags.

Recent research in OTFTs has focused on small-molecule organic semiconductors, such as α-6T, metallo-phthalocyanines and naphthalene derivatives, and aromatic hydrocarbon pentacenes have shown promising electrical performance. For example, with aromatic hydrocarbon pentacene, mobilities $\sim$1 cm^2/Vs and on/off current ratios $\sim 10^8$ have been obtained (37). However, they have large subthreshold slopes and large positive threshold voltages (37). One reason for the large subthreshold slopes may be the tendency of the small-molecule materials to form molecular crystals, resulting in a poor gate dielectric semiconducting polymer interface (37).

Table 1 is a summary of various semiconducting polymers used in TFTs with their mobilities listed for comparison. Examples of gate electrodes are nickel, aluminum, heavily doped silicon, and palladium deposited by evaporation or sputtering. For source and drain terminals, palladium, aluminum, gold, or chromium deposited by evaporation or sputtering, can be used. For gate dielectrics, thermally grown or sputtered silicon dioxide is typically used, and borosilicate glass, silicon, or plastic which offers better thermomechanical compatibility with the organic semiconductor, are used as substrate materials.

For efficient electronic transport in OTFTs, first, the relative orientation of the organic molecules on the substrate is most important. For the most efficient electronic transport, the direction of the π–π molecular overlap should be the same as the source and drain direction, that is, perpendicular to the substrate for TFTs. For pentacene and α-6T, this is the case. Second, the molecules must be packed in the unit cell in such a way that the π–π molecular orbitals overlap. Examples of this overlap are in polythiophenes where the molecular chains are coplanar and parallel to one another, so there is good overlap of their molecular orbitals. In α-6T and other thiopene-based organic materials, the chain molecules are arranged in a herringbone pattern, with the molecular chains parallel to one another. Third, the growth habit of the molecules, which leads to macroscopic crystals and polycrystalline aggregates, that is, the morphology of the films, is also important. Note, however, that the crystal's growth habit is to a large extent an inherent characteristic of each organic material. The preferable morphology is larger, perfect flat crystals.

One way to accomplish perfect flat crystals might be vacuum evaporation onto heated substrates. Solution casting has also been proposed as a fabrication method for realizing perfect flat crystals (41,42). In MISFETs, electrical characteristics are a convolution of the intrinsic transport properties of the oligomer material, which is related to its molecular stacking with extrinsic influences, the extent of grain boundaries, and the roughness of the interfaces with the source and drain contacts, and the gate dielectric layer.

Flash evaporation is used to deposit organic films to avoid problems with thermal decomposition of material being evaporated. However, it results in poor molecular ordering which leads to poor mobility. Fused-ring, small-molecule aromatic hydrocarbon pentacenes purified by vacuum gradient sublimation and deposited by vacuum evaporation onto substrates at room temperature or elevated temperatures are used in making TFTs. Sublimation and solution- or melt-processing are also easy fabrication techniques that are used. Patterning of organic materials is problematic because typical photolithographic processes lead to large changes in device characteristics.

Table 1. Summary of Various Semiconducting Polymers Used in MISFETs and Their High Mobilities

Material Used as Semiconductor in MISFETs	Mobility, cm^2/Vs
Polythiophene	10^{-5}
Polyacetylene, poly(3-hexylthiophene)	10^{-4}
Poly(3-alkylthiophene) (P3AT)	10^{-3}
Naphthalene tetracarboxylic dianhydride (NTDCA)	0.01
α-Hexathienylene (α-6T) with SiO_2 gate insulator	0.01 to 0.03
Copper phthalocyanine (Cu-Pc)	0.02
α,ω-Hexathiophene	0.03
Poly(3-hexylthiophene)	0.045
α,ω-Dihexylhexathiophene (DH6T)	0.13
Poly(thienylene vinylene)	0.22
C_{60}	0.3
Pentacene	1.3

PHOTOVOLTAIC CELLS, PHOTODIODES, AND METAL/ ORGANIC SEMICONDUCTOR JUNCTIONS

The need to develop inexpensive renewable energy sources continues to stimulate much research into new approaches to produce low-cost, energy-efficient photovoltaic devices, capable of generating a voltage as a result of exposure to radiation. Because of this, much effort is being expended in developing organic semiconductor-based photovoltaic cells and also photodiodes. Polymer photodiodes (devices that generates an electric signal in response to electromagnetic radiation) possess several attractive features (43). They are relatively insensitive to temperature variations (photosensitivity decreases by a factor of 2 from 300 K to 80 K), can be fabricated in large areas in unusual shapes, for example, on a hemisphere to couple with an optical system, by processing from solution at room temperature, and they are flexible.

Linear polymer photodiode arrays and image sensors have been produced. These large area, low-cost sensors can be used in a variety of applications industrial automation, office and consumer electronics, and biomedical instruments (44). They also exhibit a relatively flat response over a broad spectral range above the energy gap of the active material. Band-gap engineering in organic semiconductors is relatively easier than in inorganic semiconductors. For example, the energy gap of PPV can be tuned from 2.5 eV to 1.7 eV by adding side chains or functional groups.

Photodiodes can also be made by reverse biasing the LEP structures, such as Al or Ca/MEH-PPV/ITO or Ca/PPV/ITO layered thin films. Photovoltaic characteristics of Ca/MEH-PPV/ITO structures with short-circuit current density J_{SC} of 6 μA/cm^2 and open-circuit voltage V_{OC} of 1.6 V at an illumination of 20 mW/cm^2 at 430 nm broadband radiation, have been obtained. At -10V, the photodiode sensitivity is 45 mA/W to 90 mA/W under illumination of 1 μW/cm^2, which corresponds to a quantum yield of $\sim$20%. Using poly(3-octylthiophene) (P3OT) as the organic semiconductor, higher photosensitivities of 0.2 are obtained (2).

Photodiodes using the photovoltaic effect have also been investigated in PPV and MEH-PPV, one of the soluble derivatives of PPV, poly(3-alkylthiophene) (P3AT), tetrathiafulvalene (TTF), and buckminsterfullerene C_{60}. C_{60} is preferable to PPV because of its higher mobility, higher electron affinity, and higher ionization energy (45). A schematic representation of a photovoltaic cell structure is shown in Fig. 11. With photoexcitation, excitons are formed in the PPV, and they then diffuse to the PPV/C_{60} interface where they are ionized. The exciton diffusion range is $\sim$7 nm. The SiO strips define the active area of the diode and prevent the formation of a short circuit between the two electrodes when they are contacted to.

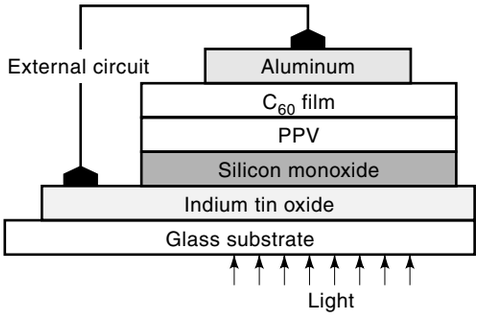

Figure 11. Simple schematic diagram of a two-layer (PPV/C_{60}) heterojunction photovoltaic diode. The C_{60} has more favorable electron-transporting characteristics than PPV, and thus it enhances the photovoltaic device's efficiency.

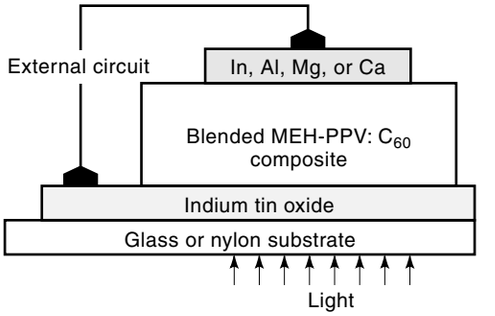

Figure 12. Simple schematic diagram of a photovoltaic cell fabricated with a blended MEH-PPV: C_{60} heterojunction material.

The current-voltage characteristics of this heterojunction photovoltaic device are those of a rectifying contact with a forward bias (ITO positive) turn-on voltage of 0.9 V. This device gives a peak quantum efficiency (electrons collected per incident photon) of 9% under short-circuit conditions and an illumination of intensity 0.1 mW/cm^2. The aluminum electrode acts as a reflecting layer for light, so the light reenters the PPV layer, and the relative phases of the forward and returning waves depend on the thickness of the C_{60} layer. By tuning the thickness of C_{60} to optimize constructive interference at the interface, and also by optimizing the PPV thickness, the quantum yields may be increased.

Photovoltaic cells (46–49) can also be made by blending a semiconducting polymer (MEH-PPV) as a donor (D) with buckminsterfullerene C_{60} as an acceptor (A) to form an interpenetrating phase-separated D–A network. Because any part of the composite is just a few nm from a D–A interface, the composite is in effect a bulk D–A heterojunction material. The structure of this photovoltaic cell is shown in Fig. 12.

In reverse bias, these "blended" devices are excellent broadband photodetectors: at -2 V to -5 V, the sensitivity is 0.2 to 0.3 A/W, and energy conversion efficiency η_E is 50 to 80% at 20 mW/cm^2 and 430 nm. These results are comparable to the 0.2 A/W photosensitivity of UV-enhanced silicon photodetectors at 430 nm. When operated as a photovoltaic cell, its characteristics are as follows: carrier collection efficiency $\eta_C \sim 29\%$; η_E of 2.9%; J_{SC} of 2 mA/cm^2 at 20 mW/cm^2 and 430 nm. At lower illumination levels of 10 μW/cm^2, $\eta_C \sim 45\%$, and $\eta_E \sim 3.3\%$. These results are significantly better that photovoltaic diodes made with MEH-PPV alone, and they are close to results from amorphous films of inorganic semiconductors (45).

As with OLEDs and LEPs, care must be taken in depositing semiconducting polymer film as incorporation of molecular oxygen into the film usually leads to low quantum yields. This may assist the process of charge separation, with electrons being trapped by the molecular oxygen, leaving holes as the mobile carriers.

Schottky diodes (50) for possible electronic applications have been made by evaporating indium contacts on poly(3-hexylthiophene) (P3HT), and they have rectification ratios of

1000 : 1. Other semiconducting polymers used to make Schottky diodes include polyacetylene, polythiophne (PT), poly(3-methylthiophene) (P3MT), and poly(3-alkylthiophene) (P3AT) deposited on ITO-coated glass, for example.

Schottky barrier solar cells using semiconductive polyacetylene $(CH)_x$ films which can be doped with donors or acceptors to yield p–n junctions suitable for solar cell devices have been fabricated. $(CH)_x$ is very suitable for solar cell applications because its absorption spectrum is close to the solar spectrum, it has a very large absorption coefficient (10^5 to 10^6 cm^{-1}), and its band gap is around 1.5 eV, at which optimum energy conversion efficiency is obtained.

For low-cost solar cells, a Schottky barrier device is preferable to a p–n junction. Its structure is Al/$(CH)_x$/Au. Its rectification in the dark for both solar cell or photovoltaic applications is significantly influenced by the surface condition of the $(CH)_x$ film. As a solar cell, incident light intensity of 7 mW/cm^2 results in an open circuit voltage of 0.32V or a short-circuit current density of 35 $\mu A/cm^2$ for a conversion efficiency of ~1.1%. Other results are a power efficiency of 4% under monochromatic light at 470 nm at low level of 0.8 $\mu W/cm^2$. The power efficiency decreases as the light intensity increases. At low illumination levels, power conversion is a linear function of the illumination because the primary carrier generation mechanism is a direct band-to-band process with a quantum yield of ~1. At higher illumination, a sublinear dependence of power efficiency is obtained, most likely due to bimolecular recombinations.

Finally, Schottky barrier diodes with poly(3-methylthiophene) have been studied over a range of temperatures and frequencies. These devices have proven very useful in studying localized states in the polymer band gap. Capacitance-voltage results suggest the presence of two acceptor states in the band gap. This is useful in understanding electrical transport in these materials so that improved and optimized devices for target applications can be fabricated.

REFERENCES

1. Z. Xie et al., Electrical characteristics of poly(3-hexylthiophene) thin film MISFETs, *Can. J. Phys.,* **70**: 1171–1177, 1992.
2. G. Yu, High performance photonic devices made with semiconducting polymers, *Synth. Met.,* **80** (2): 143–150, 1996.
3. C. C. Wu et al., Integration of organic LEDs and TFTs onto flexible and lightweight metal foil substrates, *IEEE Trans. Electron Device Lett.,* **18**: 609–612, 1997.
4. A. Dodabalapur et al., Microcavity effects in organic semiconductors, *Appl. Phys. Lett.,* **64**: 2486–2488, 1994.
5. A. Dodabalapur et al., Organic field-effect transistors, *Science,* **269**: 1560–1562, 1995.
6. X. Lu et al., Studies of polymer-based field effect transistors, *Proc. Can. Conf. Electr. Comput. Eng.,* Vancouver, Canada, 14–17 September 1993, pp. 814–816.
7. F. Garnier et al., An all-organic "soft" thin film transistor with very high carrier mobility, *Adv. Mater.,* **29** (12): 592–594, 1990.
8. G. Yu and A. J. Heeger, High efficiency photonic devices made with semiconducting polymers and their applications to emissive displays and image sensors, *Proc. Int. Semicond. Device Res. Symp.,* Charlottesville, VA, 1997, pp. 421–424.
9. M. Remmers et al., The optical, electronic and electroluminescent properties of novel poly(*p*-phenylene)-related polymers, macromolecules, **29**: 7432–7445, 1996.
10. G. Yu, C. Zhang, and A. J. Heeger, Dual function semiconducting polymer devices: Light emitting and photodetecting diodes, *Appl. Phys. Lett.,* **64**: 1540, 1994.
11. P. E. Burrows et al., Reliability and degradation of organic light emitting diodes, *Appl. Phys. Lett.,* **65**: 2922–2924, 1994.
12. D. R. Baigent, P. G. May, and R. H. Friend, Emission characteristics of two-polymer layer electroluminescent devices operating under various duty cycles, *Synth. Met.,* **76** (1–3): 149–152, 1996.
13. S. Karg et al., Increased brightness and lifetime of polymer light emitting diodes with polyaniline anodes, *Synth. Met.,* **80**(2): 111–117, 1996.
14. D. R. Baigent et al., Electroluminescence in conjugated polymers: Excited states in cyano-derivatives of poly(*p*-phenylenevinylene), *Synth. Met.,* **80** (2): 119–124, 1996.
15. C. C. Wu et al., Integrated three-color organic light emitting diodes, *Appl. Phys. Lett.,* **69**: 3117–3119, 1996.
16. P. E. Burrowes et al., Achieving full-color organic light-emitting devices for lightweight, flat-panel displays, *IEEE Trans. Electron Devices,* **44**: 1189–1203, 1997.
17. Y. Hamada, The development of chelate metal complexes as organic electroluminescent material, *IEEE Trans. Electron Devices,* **44**: 1208–1217, 1997.
18. C-C. Wu et al., Efficient organic electroluminescent devices using single-layer doped polymer thin films with bipolar current transport abilities, *IEEE Trans. Electron Devices,* **44**: 1269–1281, 1997.
19. J. H. Burroughes, C. A. Jones, and R. A. Friend, Polymeric semiconductor devices, *Synth. Met.,* **2** (1–2): C735–C745, 1989.
20. K. Itano, et al., Fabrication and performance of a double-layer organic electroluminescent device using a novel starburst molecule, 1,3,5-tris[*N*-(4-diphenylaminophenyl)phenylamino]benzene, as a hole transport material and tris(8-quinolinolato)aluminum as an emitting material, *IEEE Trans. Electron Devices,* **44**: 1218–1221, 1997.
21. Y. Yang and Q. Pei, Electron injection polymer for polymer light emitting diodes, *J. Appl. Phys.,* **77**: 4807–4809, 1995.
22. T. A. Fisher et al., Electroluminescence from a conjugated polymer microcavity structure, *Appl. Phys. Lett.,* **67**: 1355–1357, 1995.
23. D. G. Lidzey et al., Characterization of the emission from a conjugated polymer microcavity, *Synth. Met.,* **76** (1–3): 129–132, 1996.
24. J. Gruner, F. Cacialli, and R. H. Friend, Emission enhancement in single layer conjugated polymer microcavities, *J. Appl. Phys.,* **80**: 207–215, 1996.
25. N. Tessler, G. J. Denton, and R. H. Friend, Lasing from conjugated polymer microcavities, *Nature,* **382** (6593): 695–697, 1996.
26. T. Nakayama, Y. Itoh, and A. Kakuta, Organic photo- and electroluminescent devices with double mirrors, *Appl. Phys. Lett.,* **63**: 594–595, 1993.
27. M. Berggren et al., Polymer light emitting diodes placed in microcavities, *Synth. Met.,* **76** (1–3): 121–123, 1996.
28. A. Dodabalapur et al., Organic heterostructure field-effect transistors, *Science,* **269**: 1560–1562, 1995.
29. G. Horowitz et al., All-organic field effect transistors made of π-conjugated oligomers and polymeric insulators, *Synth. Met.,* **54** (1–3): 435–445, 1993.
30. F. Garnier et al., All-polymer field-effect transistor realized by printing techniques, *Science,* **265**: 1684–1686, 1994.
31. M. S. A. Abdou et al., Reversible charge transfer complexes between molecular oxygen and poly(3-alkylthiophenes), *Adv. Mater.,* **6** (11): 838–841, 1994.
32. A. R. Brown et al., Logic gates made from polymer transistors and their use in ring oscillators, *Science,* **270**: 972–974, 1995.
33. M. S. A. Abdou et al., The nature of impurities in π-conjugated polymers prepared by ferric chloride and their effect on the elec-

trical properties of metal-insulator-semiconductor structures, *Chem. Mater.,* **7** (4): 631–641, 1995.

34. J. G. Laquindanum et al., n-Channel transistor materials based on naphthalene frameworks, *J. Am. Chem. Soc.,* **118**: 11331–11332, 1996.
35. J. G. Laquindanum, H. E. Katz, and Z. Bao, Complementary circuits with organic transistors, *Appl. Phys. Lett.,* **69**: 4227–4229, 1996.
36. C. P. Jarrett et al., Transport studies in C_{60} and C_{60}/C_{70} thin films using metal-insulator-semiconductor field-effect transistors, *Synth. Met.,* **77** (1–3): 35–38, 1996.
37. Y. Y. Lin et al., Pentacene-based organic thin film transistors, *IEEE Trans. Electron Devices,* **44**: 1325–1331, 1997.
38. T. N. Jackson et al., Organic thin film transistors, *Proc. Int. Semicond. Device Res. Symp.,* Charlottesville, VA, December 1997, pp. 409–412.
39. A. J. Lovinger et al., Organic and polymeric thin film transistors and their underlying structural requirements, *Proc. Int. Semicond. Device Res. Symp.,* Charlottesville, VA, December 1997, pp. 413–416.
40. C. D. Dimitrakopoulos et al., Field-effect transistors comprising molecular beam deposited α,o-hexylthienylene and polymeric insulator, *Synth. Met.,* **92**: 47–52, 1998.
41. C-T. Kuo, S-Z. Weng, and R-L. Huang, Field-effect transistor with polyaniline and poly(2-alkylaniline) thin film as semiconductor, *Synth. Met.,* **88**: 101–107, 1997.
42. Z. Bao et al., High-performance plastic transistors fabricated by printing techniques, *Chem. Mat.,* **9**: 1299–1301, 1997.
43. J. Tsukamoto et al., Characteristics of Schottky barrier solar cells using polyacetylene $(CH)_x$), *Synth. Met.,* **4** (3): 177–186, 1982.
44. G. Yu, K. Pakbaz, and A. J. Heeger, Semiconducting polymer diodes: Large size, low cost photodetectors with excellent visible-ultraviolet sensitivity, *Appl. Phys. Lett.,* **64**: 3422–3424, 1995.
45. G. Yu et al., Polymer photovoltaic cells: Enhanced efficiencies via a network of internal donor-acceptor heterojunctions, *Science,* **270**: 1789–1791, 1995.
46. S. Glenis et al., Electrochemically grown polythiophene and poly(3-methylythiophene) organic photovoltaic cells, *Thin Solid Films,* **111** (2): 93–103, 1984.
47. P. Fedorko and J. Kanicki, Electrical and photovoltaic properties of metal contacts to *trans* -polyacetylene, *Thin Solid Films,* **113** (1): 1–14, 1984.
48. D. Fichou et al., Schottky junctions based on vacuum evaporated films of thiophene oligomers, *Synth. Met.,* **28** (1–2): C729–C734, 1989.
49. J. J. M. Halls et al., Exciton diffusion and dissociation in a poly(*p*-phenylenevinylene)/C_{60} heterojunction photovoltaic cell, *Appl. Phys. Lett.,* **68**: 3120–3122, 1996.
50. J. J. M. Halls et al., Exciton dissociation at a poly(*p*-phenylenevinylene)/C_{60} heterojunction photovoltaic cell, *Synth. Met.,* **77**: 277–280, 1996.
51. J. Birgerson et al., Conjugated polymer surfaces and interfaces: A mini-review and some new results, *Synth. Met.,* **80** (2): 125–130, 1996.

M. JAMAL DEEN
Simon Fraser University